

Bulletin 21 of the International Leonid Watch: Global analysis of visual observations of the 2006 Leonid meteor shower

Rainer Arlt¹ and Geert Barentsen²

Visual observations of the 2006 Leonid meteor shower as collected in the Visual Meteor Database (VMDB) are investigated. The Leonids exhibited a short-lived activity peak on November 19, 2006, at $4^{\text{h}}46^{\text{m}} \pm 6$ m UT. The maximum ZHR was 75 ± 8 . The activity peak coincides with a maximum of the population index of $r = 2.46 \pm 0.14$. The outburst is associated with the encounter with the 2-revolution dust trail of the parent comet 55P/Tempel-Tuttle.

1 Predictions and observations

A number of activity peaks of the Leonid meteor shower has been observed since 1998. Most of these peaks are associated with particular dust trails ejected at individual perihelion passages of the parent comet, 55P/Tempel-Tuttle. The simulation of the evolution of these dust trails has been used successfully to predict the activity peaks of the Leonids up to several years in advance. A prediction for 2006 was already included in the set of predictions by McNaught & Asher (1999a). They identified the dust trail ejected during the 1932 return of the comet to come close to the Earth in 2006 and found an encounter time of November 19, $04^{\text{h}}45^{\text{m}}$ UT (solar longitude $\lambda_{\odot} = 236^{\circ}613$ referring to equinox J2000.0). A tentative maximum ZHR of 150 was given for the prediction. Little has changed after the refinement of the models since. A dust trail integration by Lyytinen and van Flandern (2000) led to an encounter time of $04^{\text{h}}48^{\text{m}}$ UT ($\lambda_{\odot} = 236^{\circ}615$) and a peak ZHR estimate of 50. The more recent prediction by Maslov (2006) gives a peak time of $4^{\text{h}}55^{\text{m}}$ UT ($\lambda_{\odot} = 236^{\circ}620$) for the 1932 trail. He also computed an encounter time of November 20, $6^{\text{h}}28^{\text{m}}$ UT for the 19-revolution trail of 1366, but with a pessimistic expected ZHR of 1. The solar longitude of that peak would be $\lambda_{\odot} = 237^{\circ}694$.

Weather at many places in central, western, and southern Europe permitted observations; it was probably a better-than-average November 18/19 for astronomical purposes, but fog was a problem for a number of sites. The Meteosat image in Fig. 1 gives a rough impression of the weather situation near midnight. Eastern European observers had to stop early because of the beginning of twilight and could not cover the entire period of interest. In total, 93 observers reported 2801 Leonids seen in 297.54 h of observing time. We are very grateful to

Harshad Abhyankar (ABHHA, $1^{\text{h}}90$, 4), Ioan Agavriiloaiei (AGAIO, $1^{\text{h}}15$, 6), Karl Antier (ANTKA, $4^{\text{h}}33$, 65), Julia Babina (BABJL, $1^{\text{h}}08$, 10), Jaydeep Belapure (BELJA, $2^{\text{h}}00$, 13), Felix Bettonvil (BETFE, $2^{\text{h}}92$, 34), Sushrut Bhanushali (BHASU, $1^{\text{h}}00$, 12), Andreas Buchmann (BUCAN, $3^{\text{h}}18$, 70), Hans Buchholtz (BUCHA, $0^{\text{h}}64$, 7), Vasko Cacanowski (CACVA, $4^{\text{h}}03$, 40), Ed Cannon (CANED, $4^{\text{h}}18$, 39), Jakub Cerny (CERJA, $1^{\text{h}}51$, 12), Igor Chalenko (CHAIG, $2^{\text{h}}41$, 9), Sarthak Chandra (CHASR, $0^{\text{h}}83$, 7), Lorenzo Comolli (COMLO, $2^{\text{h}}27$, 41), Tim Cooper (COOTI, $3^{\text{h}}41$, 8), Nadka Dankova (DANNA, $2^{\text{h}}15$,

17), Sarthak Dasadia (DASSA, $4^{\text{h}}50$, 22), Samer Derbi (DERSA, $2^{\text{h}}99$, 22), Onkar Dixit (DIXON, $1^{\text{h}}50$, 19), Jaka Dobaj (DOBJA, $1^{\text{h}}79$, 37), Kenneth Drake (DRAKE, $0^{\text{h}}92$, 11), Shawn Dvorak (DVOSH, $0^{\text{h}}50$, 1), Shlomi Eini (EINSH, $3^{\text{h}}30$, 55), David Entwistle (ENTDA, $1^{\text{h}}08$, 7), Eric Flescher (FLEER, $3^{\text{h}}18$, 10), Mitja Govedic (GOVMI, $2^{\text{h}}00$, 8), Robin Gray (GRARO, $4^{\text{h}}05$, 18), Peter Greskovic (GREPE, $1^{\text{h}}51$, 6), Pavol Habuda (HABPA, $4^{\text{h}}29$, 41), Torsten Hansen (HANTO, $2^{\text{h}}68$, 64), Roberto Haver (HAVRO, $2^{\text{h}}58$, 39), Martin Hörenz (HORMJ, $2^{\text{h}}08$, 19), Petr Horalek (HORPT, $3^{\text{h}}55$, 55), Sagar Joglekar (JOGSA, $1^{\text{h}}50$, 8), Carl Johannink (JOHCA, $13^{\text{h}}08$, 218), Kearn Jones (JONKR, $2^{\text{h}}00$, 10), Bhargav Joshi (JOBH, $2^{\text{h}}77$, 6), Javor Kac (KACJA, $5^{\text{h}}38$, 74), Amol Kankariya (KANAM, $1^{\text{h}}00$, 4), Roy Keeris (KEERO, $2^{\text{h}}13$, 11), Prakash Khatri (KHAPR, $1^{\text{h}}08$, 4), Gyula Kiss (KISGY, $1^{\text{h}}75$, 17), André Knöfel (KNOAN, $3^{\text{h}}87$, 28), Judith de Koster (KOSJU, $1^{\text{h}}95$, 6), Ralf Koschack (KOSRA, $1^{\text{h}}60$, 27), Jakub Koukal (KOUJA, $14^{\text{h}}50$, 85), Richard Kramer (KRARI, $0^{\text{h}}57$, 3), Ashish Kuvelkar (KUVAS, $1^{\text{h}}66$, 4), Jens Lacorne (LACJE, $2^{\text{h}}89$, 29), Anna S. Levina (LEVAN, $6^{\text{h}}99$, 101), Hartwig Lüthen (LUTHA, $1^{\text{h}}89$, 23), Tony Markham (MARTO, $6^{\text{h}}44$, 11), Paul Martsching (MARPA, $13^{\text{h}}50$, 40), Pierre Martin (MARPI, $1^{\text{h}}22$, 11), Alastair McBeath (MCBAL, $8^{\text{h}}67$, 31), Mukul Mhaskey (MHAMU, $3^{\text{h}}00$, 18), Koen Miskotte (MISKO, $18^{\text{h}}95$, 300), Sirko Molau (MOLSI, $0^{\text{h}}88$, 21), Sabine Wächter (MORSA, $2^{\text{h}}08$, 25), Yousef Mteir (MTEYO, $1^{\text{h}}83$, 12), Sven Näther (NATSV, $1^{\text{h}}15$, 6), Martin Nedved (NEDMA, $3^{\text{h}}85$, 27), Daniel van Os (OSVDA, $2^{\text{h}}08$, 16), Robert Pomohaci (POMRO, $1^{\text{h}}00$, 22), Nilesh Puntambekar (PUNNI, $3^{\text{h}}15$, 13), Tushar Purohit (PURTU, $1^{\text{h}}50$, 18), Jürgen Rendtel (RENJU, $4^{\text{h}}68$, 37), Basheer Saleh (SALBA, $1^{\text{h}}50$, 7), Dan Self (SELDA, $1^{\text{h}}01$, 43), Jonathan Shanklin (SHAJO, $4^{\text{h}}89$, 46), Vladimir Slusarenko (SLUVL, $2^{\text{h}}41$, 5), Ulrich Sperberg (SPEUL, $2^{\text{h}}85$, 14), David Stine (STIDA, $3^{\text{h}}00$, 6), Boris Stoilov (STOBO, $7^{\text{h}}31$, 29), Martin Stojanovski (STOMT, $4^{\text{h}}34$, 49), Wesley Stone (STOWE, $1^{\text{h}}50$, 9), Magda Streicher (STRMA, $1^{\text{h}}62$, 7), Oana Suciuc (SUCOA, $2^{\text{h}}99$, 23), Khaled Tell (TELKH, $3^{\text{h}}49$, 16), Cristina Tinta (TINCR, $2^{\text{h}}04$, 8), Rafaél R. Torregrosa Soler (TORRQ, $2^{\text{h}}00$, 21), Josep M. Trigo Rodríguez (TRIJO, $2^{\text{h}}15$, 30), Blanca Troughton Luque (TROBL, $1^{\text{h}}68$, 9), Shigeo Uchiyama (UCHSH, $2^{\text{h}}00$, 10), Michel Vandeputte (VANMC, $11^{\text{h}}94$, 268), Valentin Velkov (VELVA, $2^{\text{h}}72$, 22), Jan Verfl (VERJX, $1^{\text{h}}51$, 12), Frank Wächter (WACFR, $1^{\text{h}}95$, 21), Graham Winstanley (WINGR, $2^{\text{h}}35$, 19), Kim S. Youmans (YOUKI, $3^{\text{h}}00$, 8), Weizhou Zeng (ZENWE, $3^{\text{h}}19$, 17), Wen Zhou (ZHOWE, $2^{\text{h}}00$, 8),

coming from

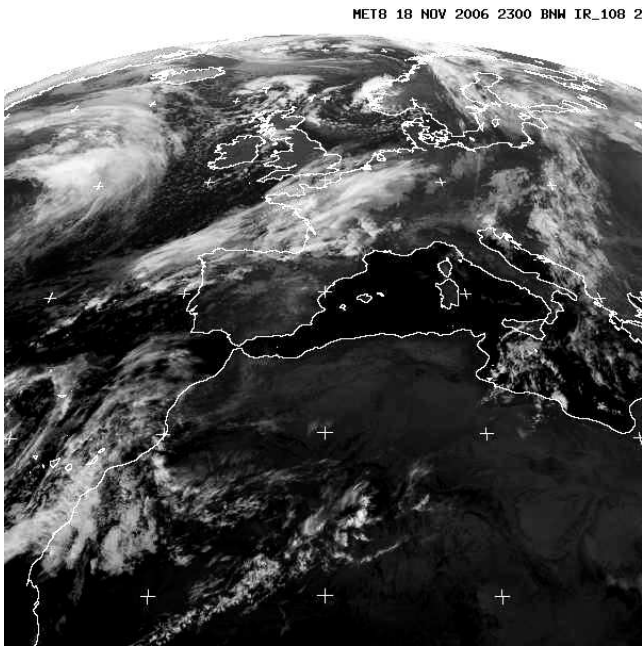


Figure 1: Meteosat infrared image of 2006 November 18, 23^h UT showing the European weather situation a few hours before the expected Leonid peak (copyright 2006 EUMETSAT, <http://www.eumetsat.int>).

Australia, Belgium, Bulgaria, Canada, China, Czech Republic, Denmark, France, Germany, Hungary, India, Israel, Italy, Japan, Jordan, Lithuania, Macedonia, the Netherlands, Portugal, Romania, Slovakia, Slovenia, South Africa, Spain, Switzerland, the UK, the Ukraine, and the USA

for their observing efforts and swift reporting of the data.

2 Data treatment

2.1 Live activity profile

A large fraction of observations was submitted very quickly through an online report form implemented by Geert Barentsen as a step on the way to an online global meteor database. For the moment, the online form script sends a message to RA for manual input in the Visual Meteor Database (VMDB), which is at present the largest data set of visual meteor shower activity and magnitude data. Since the form script also checks the data on plausibility, it computes various quantities from the data such as the radiant elevations. These could be employed to derive values of zenithal hourly rates (ZHR) directly on the web server which were averaged every minute for a ZHR profile shown on the IMO web site. The live graph was in fact computed in exactly the same way as the IMO shower circulars are usually created, which are distributed on a few mailing lists, yet without manual interference. The preliminary profile as based on 61 observers who made use of the online report form is shown in Fig. 2 as of November 30, 2006.

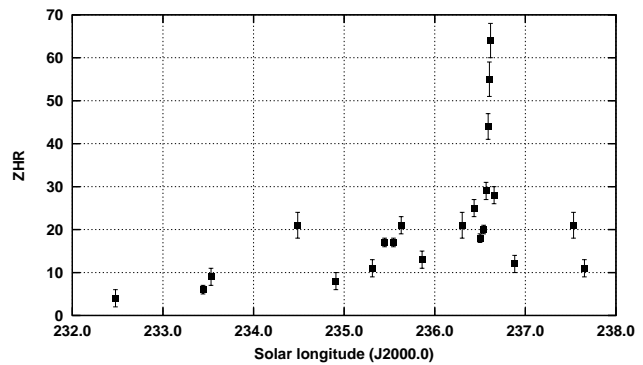


Figure 2: Preliminary ZHR profile of the 2006 Leonids automatically derived from observations submitted through the online report form until November 30, 2006. All solar longitudes in this and the following graphs refer to equinox J2000.0.

2.2 Population index

Since the ZHR implies a correction of the shower meteor number seen under an actual limiting magnitude to a standard limiting magnitude of +6.5, we need to know the population index r of the shower before any computation of the ZHR. It represents the particle size distribution in the meteoroid stream and will naturally depend on time. Our first step towards a final activity profile of the 2006 Leonids is the computation of the Leonid population index profile. A total of 286 magnitude distributions containing 2619 Leonid magnitudes was used to construct the profile. An adaptive-bin-size algorithm goes through the data and forms temporal bins with roughly the same number of meteors in each bin.

The bin-size algorithm is explained below in detail when we describe the ZHR averaging. The population index is the factor by which the true meteor number grows when going to the next-fainter magnitude class. The true meteor number is defined as not being affected by reduced perception capabilities of the observer for fainter meteors. In a diagram of the logarithms of true meteor numbers versus magnitude class, the points should form a straight line (power law). A first guess would determine the regression line through the points, but another way of getting from meteor magnitudes to the population index yields half as large error margins: the population index is based on the average magnitude difference to the limiting magnitude for each individual meteor. For any given population index r , one can simulate many magnitude distributions which also involve the perception probabilities for any meteor magnitude as published by Koschack & Rendtel (1990). These simulations deliver the mean magnitude difference from the limiting magnitude as well as – from the diversity of simulated distributions – the error margins. A conversion table of mean magnitude differences to r is given in Arlt (2003).

Since the mean magnitude difference is independent of the limiting magnitude, we can group different observers and observations into one average and obtain

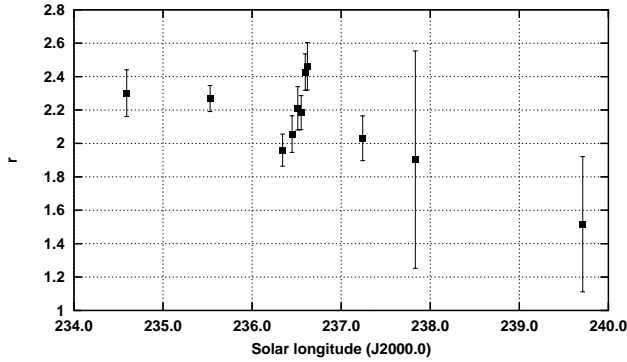


Figure 3: Population index profile of the 2006 Leonids as derived from visual observations.

an average r for a given period. The resulting population index profile is shown in Fig. 3. The population index evolution starts with a value near $r = 2.3$ and ends up with a value of $r = 1.5$, but with a very large uncertainty. We can interpret the profile such that a general decrease throughout the activity period of the Leonids is observed, while a short-lived peak of high r is superimposed to this general trend. The peak is as high as $r = 2.46 \pm 0.14$ and is not typical for cometary shower material which is in its orbit for many revolutions after ejection already. The high population index is compatible with material ejected only a few revolutions ago and thus with a dust trail ejected in 1932.

The time of the peak is $\lambda_{\odot} = 236^{\circ}61' \pm 0^{\circ}01'$ or November 19, $04^{\text{h}}41^{\text{m}} \pm 15 \text{ m}$ UT. The uncertainty is relatively large, because very many meteors are required to obtain small error margins. A profile with finer time resolution would result in much larger error bars and does not point significantly to a more precise time.

The problem with interpreting the high r as an actual peak is the missing declining branch. The increasing r may not be due to the young material, but simply due to a radiant-elevation effect, since nearly all observers who recorded the corresponding meteor magnitudes were located in western Europe and saw the same behaviour of the radiant rising towards the end of the night.

In an experiment, we computed the population index from observations for which the radiant elevation was in the interval from 40° to 60° at the middle of the observing period. The radiant height dependence should be reduced. Fig. 4 shows the corresponding profile; the r -peak near the expected dust trail encounter is still present. Note that the r -value one day earlier is also high, and we cannot exclude that a radiant-height effect is superimposed to the real features. The original point for about $\lambda_{\odot} \approx 235^{\circ}5'$ in the profile of Fig. 3 contained various other radiant elevations and is not that high. The error bars of the points near $\lambda_{\odot} \approx 235^{\circ}5'$ in Figs. 3 and 4 still overlap though. The same holds for the peak- r one day later.

2.3 Zenithal hourly rate

We employ a weighted averaging with the total correction coming from the stellar limiting magnitude lm ,

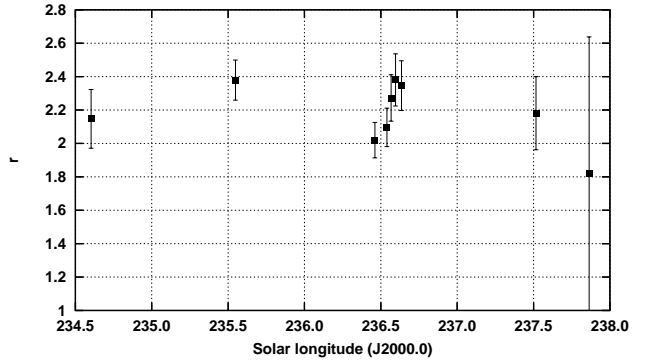


Figure 4: Population index profile of the 2006 Leonids as derived from magnitude distributions for which the radiant elevation was in the interval from 40° to 60° at the middle. Only the period near the maximum was selected here.

possible obstructions of the field of view expressed by F , the radiant elevation h_R , and the effective observing time T_{eff} . The average ZHR is given by

$$\overline{\text{ZHR}} = \left(\sum_{i=1}^N n_i + 1 \right) / \sum_{i=1}^N C_i, \quad (1)$$

where the n_i and the C_i are the number of Leonids and the total correction factors of the N individual observing periods, respectively. The total correction is computed by

$$C = \frac{r^{6.5 - lm} F}{T_{\text{eff}} \sin h_R} \quad (2)$$

The averaging is again an adaptive process where the essential input is an optimum meteor number to be comprised by each average. The activity period is divided into averaging bins each containing approximately the optimum meteor number. For the full ZHR profile, we set this number to 200 Leonids. While going through the data records in chronological order, the algorithm accumulates periods with meteors until it reaches the optimum meteor number. This defines the bin width. The width may, however, be too short for a few periods which are longer than the bin and thus not suitable. The algorithm has to search iteratively to reach the optimum meteor number in each bin without using periods that are longer than the bin. A period is considered lying in the averaging bin, if its middle is within the bin.

There are of course very few meteors far from the shower maximum, and we have to give an upper bin width as the bin might cover several days otherwise. On the other hand, if very many meteors are available, the bin width may become shorter than the typical observing period which is reported during that time, say 5 or 10 minutes. For example, the optimum meteor number may already be reached when the bin width is only 3 minutes, and the algorithm finds that it has to exclude nearly all observing periods from the bin. The optimum meteor number is then not reached and the bin width is extended until it reaches the 5-minute dura-

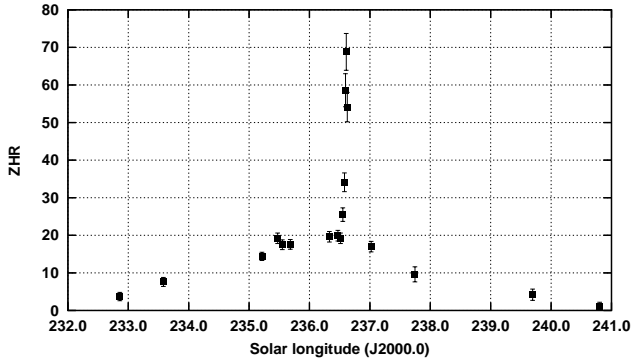


Figure 5: ZHR profile of the 2006 Leonids as derived from visual observations.

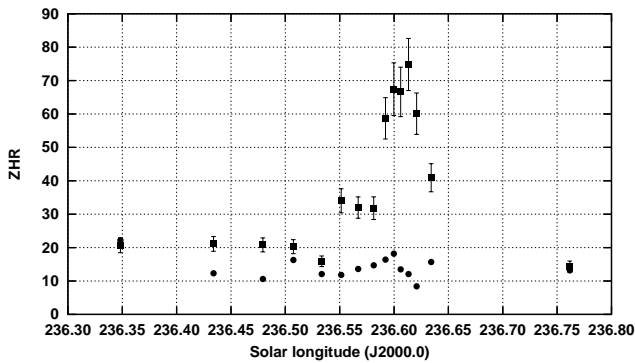


Figure 6: ZHR profile of the 2006 Leonid maximum as derived from visual observations. The temporal resolution is higher than in Figure 5. The circles are the average sporadic hourly rates for the same time bins as the ZHR. Their error bars are omitted, but are between ± 1 and ± 3 for most of the points and ± 4 for the maximum point near $\lambda_{\odot} = 236^{\circ}6$.

tion to include the periods which are actually available. The algorithm may thus flip between two solutions – a short bin with not enough meteors or a longer period with way too many meteors – without converging. This dead-lock can be prevented by setting a minimum bin width.

Because of the very uneven distribution of observations during the activity period of the 2006 Leonids, we composed the activity profile of two periods: (i) the first runs from $\lambda_{\odot} = 232^{\circ}$ to 236° (i.e. up to November 18, $\approx 14^{\text{h}}$ UT) with a maximum bin width of 8° (actually only a safety limit) and a minimum bin width of 1° ; (ii) the second averaging runs from $\lambda_{\odot} = 236^{\circ}$ to 243° with a maximum bin width of 2° and a minimum bin width of $0^{\circ}0069$ corresponding to 10 minutes. Each observing period is used only once in a bin.

Additional constraints are a maximum correction factor of

$$\frac{r^{6.5-\text{lm}} F}{\sin h_{\text{R}}} < 8 \quad (3)$$

and a minimum radiant elevation of $h_{\text{R}} > 10^{\circ}$. The observing direction is not considered, neither in terms of a correction nor in terms of a constraint. The radiant elevation correction is actually not based on h_{R} for the

middle of the observing period but is the average $\sin h_{\text{R}}$ over the observing period (Arlt, 1990). The difference to the simpler version is relatively small, but may matter as the radiant of the Leonids rises very quickly at mid- and low-latitude sites near local midnight. For averaging the ZHR, the solar longitude of the middle of the observing period is used. We are not applying any correction of the timing for the topocentric encounter of the stream as suggested by McNaught & Asher (1999b), because the shortest observing periods are about 5 minutes long, and the correction is smaller for nearly all sites.

The resulting activity profile of the 2006 Leonids is shown in Fig. 5. Two features are evident from the graph: (i) a broad background activity component with a maximum ZHR of about 20 and a full width at half-maximum of about $3^{\circ}5$ in solar longitudes corresponding to about 3.5 days, and (ii) a sharp peak at $\lambda_{\odot} = 236^{\circ}61$. At ten minutes resolution, this peak may be resolved though.

A special averaging run with increased temporal resolution was computed for the hours around the Leonid peak on November 19. The optimum meteor number is now 100, and the minimum bin width is $0^{\circ}0035$ corresponding to 5 minutes. This is the smallest reasonable bin width, since smaller periods were reported only occasionally (e.g. when time stamps were not taken regularly). The other constraints are the same as for the full profile in Fig. 5. The resulting “magnification” of the Leonid peak is shown in Fig. 6. A peak ZHR of 75 ± 8 occurred at a solar longitude of $\lambda_{\odot} = 236^{\circ}613$ or November 19, $4^{\text{h}}46^{\text{m}} \pm 6$ m UT. The error in the timing is simply taken as half the distance to the neighbouring averages, rounded to the next minute. The full uncertainty may be somewhat larger though.

The full width at half-maximum of the peak is about $0^{\circ}07$ or about 100 minutes. If one subtracts the background component of $\text{ZHR} \approx 20$, the width is even shorter, about $0^{\circ}04$ or 60 minutes.

The graph also shows the average sporadic hourly rate for each of the bins for the averaged Leonid activity points. These sporadic rates are simple averages of the individual $\text{HR} = n_{\text{spO}} r^{6.5-\text{lm}} F/T_{\text{eff}}$ for simplicity. The sporadic rates vary between 10 and 20 and show their strongest variation during the time of the Leonid peak, roughly between November 19, 4^{h} and 5^{h} UT. The general upward trend between $\lambda_{\odot} = 236^{\circ}4$ and $236^{\circ}6$ is most likely an effect of the diurnal variation of sporadic rates, but then, before the Leonid peak, the sporadic HR starts to decrease and reaches a minimum of below 10 after the Leonid peak. This is not an effect of observers at more western longitudes starting their observations at earlier local time whence lower sporadic rates. The first observation from an American location starts at $\lambda_{\odot} = 236^{\circ}651$, and there is – unfortunately – only a few minutes overlap between western European observations and northern American observations. Poorer conditions are also not an issue here for the variability of sporadic rates, as the average limiting magnitudes in Tab. 1 prove. We thus have to presume that the sporadic variability is an effect of higher uncer-

Table 1: Numerical data of the activity profile of the 2006 Leonids. Dates and solar longitudes refer to the average time of all the periods within the averaging bin. Solar longitudes refer to equinox J2000.0, N is the number of observing periods in each average, n_{LEO} is the total number of Leonid meteors involved in the average, ZHR is the zenithal hourly rate, $\overline{\text{lm}}$ is the average limiting magnitude, and r is the average population index as derived from linear interpolation in Fig. 3.

Date (UT)	λ_{\odot}	N	n_{LEO}	ZHR	$\overline{\text{lm}}$	r	
2006 Nov 15	11 ^h 29	232 °8618	7	10	3.7 ± 1.1	6.48	2.30 ± 0.14
2006 Nov 16	04 ^h 37	233 °5813	11	41	7.6 ± 1.2	6.17	2.30 ± 0.14
2006 Nov 17	19 ^h 27	235 °2130	48	168	14.4 ± 1.1	6.02	2.28 ± 0.11
2006 Nov 18	01 ^h 41	235 °4745	32	192	19.2 ± 1.4	6.16	2.27 ± 0.08
2006 Nov 18	03 ^h 30	235 °5511	25	181	17.5 ± 1.3	6.37	2.26 ± 0.08
2006 Nov 18	06 ^h 38	235 °6826	32	186	17.6 ± 1.3	6.26	2.22 ± 0.08
2006 Nov 18	22 ^h 28	236 °3483	21	85	20.7 ± 2.2	5.51	1.98 ± 0.10
2006 Nov 19	00 ^h 30	236 °4340	37	93	21.1 ± 2.2	6.18	2.04 ± 0.11
2006 Nov 19	01 ^h 35	236 °4793	37	97	20.8 ± 2.1	6.37	2.13 ± 0.12
2006 Nov 19	02 ^h 15	236 °5074	37	94	20.3 ± 2.1	6.30	2.20 ± 0.13
2006 Nov 19	02 ^h 52	236 °5335	43	96	15.9 ± 1.6	6.43	2.20 ± 0.11
2006 Nov 19	03 ^h 18	236 °5514	27	90	34.0 ± 3.6	6.30	2.20 ± 0.10
2006 Nov 19	03 ^h 40	236 °5670	29	98	32.0 ± 3.2	6.43	2.27 ± 0.10
2006 Nov 19	04 ^h 00	236 °5813	31	88	31.8 ± 3.4	6.27	2.35 ± 0.11
2006 Nov 19	04 ^h 16	236 °5921	23	90	58.7 ± 6.2	6.32	2.41 ± 0.11
2006 Nov 19	04 ^h 27	236 °5998	25	72	67.4 ± 7.9	6.32	2.43 ± 0.11
2006 Nov 19	04 ^h 36	236 °6061	26	81	66.6 ± 7.4	6.26	2.44 ± 0.12
2006 Nov 19	04 ^h 46	236 °6133	25	90	74.8 ± 7.8	6.31	2.45 ± 0.13
2006 Nov 19	04 ^h 57	236 °6208	33	93	60.1 ± 6.2	6.27	2.46 ± 0.14
2006 Nov 19	05 ^h 16	236 °6341	36	93	40.9 ± 4.2	6.23	2.45 ± 0.14
2006 Nov 19	08 ^h 18	236 °7617	14	68	14.3 ± 1.7	5.92	2.33 ± 0.14
2006 Nov 19	14 ^h 27	237 °0209	36	157	17.0 ± 1.4	6.24	2.19 ± 0.24
2006 Nov 20	07 ^h 44	237 °7474	6	21	9.6 ± 2.0	6.14	1.91 ± 0.59
2006 Nov 22	05 ^h 59	239 °6942	4	7	4.2 ± 1.5	5.89	1.58 ± 0.51
2006 Nov 23	08 ^h 23	240 °8057	2	0	1.1 ± 1.1	5.90	2.20 ± 1.74

tainty in associating meteors with showers, namely the Leonid radiant during the peak time, when increased rates, fainter meteors, and the prediction in mind may have affected the degree of objectivity of the visual observers. To which degree the Leonid ZHRs are affected is unknown.

The numerical data of the merged profiles of Fig. 5 and Fig. 6 is given in Tab. 1. Besides the ZHR profile, we also give the average limiting magnitude for each of the bins of ZHR averaging as well as the average population index which is linearly interpolated from the profile in Fig. 3 for each individual observing period. Observing conditions were generally very good, with only a few averages of $\text{lm} < +6$. The 2-revolution dust trail encounter is covered with observations with average limiting magnitude near +6.3. The last row is a typical effect of small-number statistics as 0 Leonids produce a ZHR of 1.1 which looks odd at first glance. However, the fact that zero meteors were seen, can be the result of a true rate (measured over an infinitely long time) larger than 0. The observer may have accidentally seen no meteors in the specific observing period. In statistical terms, the ZHR is the expectation value of all possible true rates which may have caused the observer to see 0 Leonids. It results from an integration over a Poissonian-like function. This gives an expectation value (“average”) for the true rate of 1 with additional

factors due to lm etc. The last line of Tab. 1 is a direct consequence of Eq. 1. The error margin is then 100%, however. The effect of the “+1 there has only negligible effect on the rest of Tab. 1, except for the last two lines.

There are not enough observing periods for the time near the second possible activity enhancement on November 20, 6^h28^m UT. About ten periods are available for the four hours around that time. There is also a substantial gap in observing data between the Spanish night time and the first period reported from the USA.

3 Conclusions

We investigated the 2006 return of the Leonid meteor shower as monitored by visual observations. The encounter with the 2-revolution dust trail ejected in 1932 is identified in both the population index as a period with a large fraction of faint meteors and in the ZHR-profile with a peak rate of 75 ± 8 at $\lambda_{\odot} = 236^{\circ}613$ or November 19, 4^h46^m ± 6 m UT. The agreement with the dust trail predictions by McNaught & Asher (1999) and Lyytinen & van Flandern (2000) is very good regarding the peak time and fairly reasonable regarding the estimate of the maximum ZHR. The maximum was composed of rather faint meteors given the population index of $r = 2.46 \pm 0.14$ at the peak time. A similar r -peak like this was found in the 1999 data near the 3-revolution dust trail encounter (Arlt et al. 1999). The

population index then climbed up to $r \approx 2.7$ during that encounter, using the same mean magnitude distance from lm technique as is used here.

Part of the increase in faint meteors at the peak time may be caused by a radiant-elevation effect which we cannot entirely eliminate. A restriction of observations to a 20° window of radiant elevations still showed the r -peak though.

We should also not forget though that a peak like this may be due to the increased alertness of the observers during the peak time, as the prediction was known to practically all participants. This would affect both the population index and the ZHR going up due to such an increased perception.

Much of the observational data is concentrated near the expected peak, while other periods are poorly covered by data. It must be noted that the absence of other peaks in the ZHR profile is no proof of their nonexistence. An analysis of a set of forward scatter counts worldwide may give indications for other enhancements.

References

- Arlt R. (1990), "Letter: The zenith correction factor", *WGN* **18**, 73–74.
- Arlt R., Bellot Rubio L., Brown P., Gyssens M. (1999), "Bulletin 15 of the International Leonid Watch: First Global Analysis of the 1999 Leonid Storm", *WGN* **27**, 286–295.
- Arlt R. (2003), "Bulletin 19 of the International Leonid Watch: Population index study of the 2002 Leonid meteors", *WGN* **31**, 77–87.
- Lyytinen E., van Flandern T. (2000), "Predicting the strength of Leonid outbursts", *Earth, Moon, and Planets* **82/83**, 149–166.
- Maslov M. (2006), <http://feraj.narod.ru/Radiants/Predictions/1901-2100eng/Leonids1901-2100eng.html>
- McNaught R.H., Asher D.J. (1999a), "Leonid dust trails and meteor storms", *WGN* **27**, 85–102.
- McNaught R.H., Asher D.J. (1999b), "Variation of Leonid maximum times with location of observer", *Meteoritics and Planet. Sci.* **34**, 975–978.